RESEARCH ARTICLE

Investigation on energy, economic, and environmental aspects of double-pass solar air heater

Rajendran Vijayakumar[1,3] · Ramalingam Vignesh Kumar[1] · Petchimuthu Madhu[2]

Abstract

Numerous research studies have found that a double-pass solar air heater (DPSAH) performs better than a single-pass solar air heater (SAH). This suggested study aims to evaluate the performance of a DPSAH setup in Southern Tamil Nadu, India. Several artificial roughness features have been incorporated into the solar black-coated absorber plate for this examination. Broken ribs with semi-circular and semi-polygonal shapes are used and explicitly tested on the absorber plate. Next, the efficiency of these rib designs is contrasted with a typical flat plate DPSAH. These studies also employ three different mass flow rates (0.01 kg/s, 0.02 kg/s, and 0.03 kg/s), enabling a thorough assessment of the DPSAH system's performance at each rate. These studies' findings demonstrate that adding artificial roughness to the solar collector plate has a beneficial effect on the turbulence of fluid flows. As a result, this innovation increases the double-pass solar air heater's (DPSAH) heat transfer rate. It is noteworthy that compared to the DPSAH with flat plates, both rib designs perform better. It is important to remember that the semi-polygonal ribs function better than the semi-circular ones. The average efficiency values for the semi-polygonal rib structure are 17.1%, 18.7%, and 19.1% greater than those seen for flat plates. These efficiency values are additionally 4.4%, 7.4%, and 8.7% higher than those attained with the semi-circular rib topologies at flow rates of 0.01 kg/s, 0.02 kg/s, and 0.03 kg/s, respectively. The study goes into considerable detail on how particular rib patterns can be advantageous economically and environmentally.

Abbreviations

A	Area (m^2)
AMC	Annual maintenance cost ($)
ASC	Annual salvage cost ($)
C	Cost of yield/litre ($/l)
C_p	Air-specific heat (J/kg K)
D_h	Hydraulic diameter (m)
DPSAH	Double-pass solar air heater
E_{sol}	Total solar radiation (kWh)
f	Friction factor
FAC	Fixed annual cost ($)
G	Total incident solar radiation (W/m^2)
h	Heat transfer coefficient (W/m^2 K)
i	Interest rate ($)
I	Solar intensity (W/m^2)
k	Thermal conductivity (W/mK)
L	Length (m)
$\dot{m}$	Mass flow rate of air (kg/m^2 s)
N_u	Nusselt number
P	Pressure drop (Pa)
PCC	Primary capital cost ($)
$\dot{Q}_{hl}$	Heat loss at the top (W)
R_e	Reynolds number
S	Salvage value ($)
SAH	Solar air heater
SFF	Sinking fund factor
TAC	Total annual cost ($)

✉ Ramalingam Vignesh Kumar
vigneshces@nec.edu.in

Rajendran Vijayakumar
vijaymech@nec.edu.in

Petchimuthu Madhu
pnpmadhu@gmail.com

1   Department of Mechanical Engineering, National Engineering College, Kovilpatti, Tamil Nadu, India

2   Department of Mechanical Engineering, Karpagam College of Engineering, Coimbatore, India

3   Present Address: Centre for Nonlinear Systems, Chennai Institute of Technology, Chennai, Tamil Nadu 600069, India

TAY	Total accumulated yield (W)
T_L	SAH total lifetime (years)
V	Inlet velocity (m/s)
V_w	Wind velocity (m/s)
η	SAH efficiency (%)
ρ	Density (kg/m^3)
σ	Stefan-Boltzmann constant (W/(m^{2}K))
ε	Glass emissivity

Introduction

In this developed world, a renewable source of energy is replacing the conventional source of energy in electrical and heat energy generation. Because of their availability and non-polluting nature, solar thermal (ST) systems are frequently used for various heating purposes. Solar air heaters are the most frequently utilised among all solar thermal systems. Solar air heaters generate the heat energy needed for drying, room heating, and industrial heating applications. Due to the system's internal flow patterns, solar air heaters are typically categorised as single-pass, double-pass, or multi-pass systems. The double-pass solar air heater is the most effective due to its high heat transmission. The performance of the double-pass solar air heater (DPSAH) system is the focus of more investigations. A modification was made to a traditional SAH with two glass covers and a double-pass mode for use in research (Wijeysundera et al. 1982). An experimental investigation discovered that double-pass SAH was 10–15% more efficient than single-pass SAH under the same operating conditions. An examination was conducted on the effectiveness of wire mesh layers in single-pass and double-pass SAH (Aldabbagh et al. 2010). For this arrangement, the double-pass SAH's efficiency range was 34–45% greater than the single pass SAH's.

Researchers investigated and contrasted the performance of various double-pass solar air heater types (Chamoli et al. 2012). They claimed that the mass flow rates and packed material influenced the performance of a DPSAH. Additionally, when the airflow rates and channel depths for the lower and upper parts of the DPSAH were equal, the thermal efficiency was at its highest. They also discovered that the recycling ratio was a critical factor influencing the DPSAH efficiency. Fin arrangements were used to evaluate the effectiveness of DPSAH (Fudholi et al. 2013). They contrasted these findings with those from flat plate configurations. The performance of DPSAH was investigated with mass flow rates between 0.01 and 0.1 kg/s. They obtained a maximum of 77% thermal efficiency for DPSAH with a finned configuration at increased mass flow rates of 0.09 kg/s.

The DPSAH was experimentally explored by employing wire mesh packing on the absorber (Ho et al. 2013). This study contributes to the revelation that using a wire mesh increases the SAH's heat transfer area by enhancing the turbulent flow within the system. As a result of this, the heat transfer rate increased significantly. Four transverse fins and 16 wire meshes between those fins were used to explore the operation of single-pass solar air heater (SPSAH) and DPSAH (Mahmood et al. 2015). They discovered that double-pass SAH outperformed SPSAH in performance for all of the investigated flow rates. The effectiveness of DPSAH with recycled air and wire mesh absorber designs was studied (Dhiman and Singh 2015). For this investigation, they varied the mass flow rate in the range of 0.01–0.025 kg/s. They conclude that the DPSAH system operates at a higher mass flow rate (0.025 kg/s) and has a maximum thermal efficiency of 80.8% when recycled air is used.

In order to analyse the thermal performance of the DPSAH, Ravi and Saini (2016a) used staggered and multi-V-shaped rib arrangements on both sides of the absorber plate. This performance was contrasted with the SPSAH. For DPSAH and SPSAH, the maximum Nusselt number to friction factor ratios were 3.4 and 2.5, respectively. Numerous C-shaped artificially created roughnesses over the black-coated solar absorber plate were used (Gabhane and Kanase-Patil 2017) to investigate DPSAH. They discovered that incorporating numerous C-shaped roughnesses on both sides of the DPSAH's solar black-coated absorber plate could achieve higher efficiency than scattered C-shaped DPSAH. They obtained values of 0.031 and 3.48 for friction factor and thermal–hydraulic performance, respectively. By combining a flat plate and turbulator arrangement, researchers evaluated and compared the effectiveness of DPSAH (Abdullah et al. 2018). For this experimentation, they preferred air mass flow rates in the range between 0.02 and 0.05 kg/s. By using these turbulators, DPSAH delivers 68% system efficiency at 0.05 kg/s, which is substantially higher than the flat plate. Four distinct setups were employed (Baig and Ali 2019) to study the double-pass SAH.

Additionally, they used paraffin wax as a storage medium, which can perform better in the winter. As per their analysis, an optimum efficiency of 97% was discovered when using four copper conduits. A number of paraffin wax-filled capsules were used to study the thermal performance of a DPSAH (Salih et al. 2019). They discovered that higher mass flow rates of air will decrease the melting temperature of wax throughout the melting process. For the DPSAH performance analysis, metallic finned tubes were filled with a phase-change material (PCM) (Sajawal et al. 2019). They discovered that the PCM RT44HC and RT18HC provided the optimum performance. DPSAH was studied by employing rectangular longitudinal fins (Murali et al. 2020). They independently used fins on the top channel and lower channel and compared the results. In this design, placing the fins on the lower channel yields the most efficiency compared to placing the fins on the top channel.

For the DPSAH performance investigation, a brand-new design called a tubular absorber was offered (Abo-Elfadl et al. 2021). For the study, they employed air mass flow rates in the ranges of 0.025, 0.05, and 0.075 kg/s. The aggregated thermal efficiencies of the DPSAH were 86% at a flow rate of 0.075 kg/s and 61.15% at a flow rate of 0.025 kg/s. Compared to SPSAH, this range increased by 23.15% and 38.4%, respectively. Conductive aluminium tubes were employed as an absorber for DPSAH (Abo-Elfadl et al. 2020). For 0.075, 0.05, and 0.025 kg/s air mass flow rates, this new arrangement provided 19.4%, 21%, and 40.3% higher efficiency than the flat plate. For the same mass flow rate of 0.025 kg/s, this arrangement also produced a temperature that was 6 °C higher than the flat plate. A wide range of DPSAH designs was investigated, and their performance parameters were reported (Kumar et al. 2020). Compared to symmetric ribs, the system with asymmetric semi-circular ribs offers improved thermal and thermo-hydraulic performance. According to the research, the curved DPSAH performed 37% more efficiently than the conventional SAH. The DPSAH was studied using V-corrugated and corrugated perforated designs (Hassan et al. 2021). The corrugated perforated plate offers the highest average efficiencies of 67.67%, 69.7%, 71.85%, and 70.8% for the investigated flow rates out of all the configurations examined. Additionally, it produces exergy efficiencies in the range of 0.78, 0.8, 89, 97, and 0.92.

To investigate the performance of the return flow SAH, the absorber plate was integrated with V-shaped baffles (Raturi et al. 2022). For their study, they employed a mass flow rate of air at 0.02 kg/s. For thisinvestigation, they used baffles on both sides of the absorber plate. The thermal efficiency of the return flow SAH with baffles was 33.70% higher than without baffles. For the investigation, DPSAH was built with and without vertical plate perforated baffles (Tandel and Modi 2022). Throughout the experiment trails, the SAH system received air from the upward and downward directions.

In comparison to the traditional DPSAH, the baffle arrangement of the DPSAH produces 6.48%, 17.10%, and 17.24% higher average output temperatures, average heat gains, and average efficiency at upward air flow. A variety of settings were used, including free convection, artificial convection, and forced convection with one side reflector, to examine the exergy and energy performance of the DPSAH (Prakash et al. 2022). The third condition had a significantly greater energy and exergy efficiency than the first two, at 86.19% and 17.617%, respectively. Airflow rates of 0.021–0.061 kg/s were used to study a DPSAH with a V groove (Hassan et al. 2022). According to their findings, increased mass flow rates resulted in higher thermal and exergy efficiencies of 88.8% and 6.6%, respectively.

A review was conducted on the packed bed DPSAH's thermal efficiency (Singh and Dhiman 2016). They discovered that only a minimal amount of work was done using artificial roughness and that employing wire mesh screens, iron scrap, etc., as a packed bed had no results. Additionally, they stated that the DPSAH may use a variety of flow patterns. The technologies, such as packed beds, corrugated absorbers, and fins available to enhance DPSAH performance, were explored (Ravi and Saini 2016b). They discovered that the DPSAH with single glazing may be utilised successfully for various solar applications. Every technology that could increase the heat transfer rate of the DPSAH was investigated (Alam and Kim 2017). They concluded from their analysis that DPSAH delivered 10–15% more efficiency than SPSAH for the same setup. They discovered a dearth of research on artificial roughness. There are more projects available on packed beds and storage components for better heat transfer.

An infrared heater and nano-absorber coating were used to test a solar dryer with triple flow (Khanlari and Tuncer 2023). According to the results, this setup offers a 40% faster drying rate than a traditional dryer. Additionally, it provided improved thermal and energetic efficiencies of 14.62–16.94% and 31.19–37.72%. Using mesh packing and nano-enhanced black paint, an experimental investigation was carried out to determine the effectiveness of an unglazed solar air heater (Sirin et al. 2023). By employing these arrangements, the author increased energy efficiency by 29.54% and 31.20%. Parallel flow solar collectors with and without recyclable aluminium cans filled with paraffin were tested (Tuncer et al. 2023a, b). They achieved 42.20–58.75% thermal efficiency and 74.03% energy efficiency as a result. Using an infrared heater and nanocoating, three vertical solar heaters were constructed and evaluated (Tuncer et al. 2023a, b). With these configurations, drying times are shortened by 43.75%, and average efficiency is increased to 21.13 and 21.62%. Aluminium cans are placed over the collector plate of a solar air collector with triple flow to facilitate testing (Tuncer and Khanlari 2023). With recyclable cans, these configurations increase exergy efficiency by 8.87 to 23.25%. A solar air heater was experimentally assessed using a spiral-formed solar collector and ceria nanoparticle coating (Khanlari et al. 2023). With and without nanocoatings, this spiral collector has average thermal efficiencies of 46.15 and 67.39%, respectively.

The literature review highlights several efforts to enhance the efficiency of solar air heaters (SAH) by utilising baffles. These baffles serve the primary function of altering the internal airflow pattern of the SAH, facilitating the mixing of lower and upper air layers and thereby creating a more significant temperature difference to enhance heat transfer. This adjustment in airflow pattern can notably augment the system's efficiency and heat transfer rate. The choice of

baffle shapes is crucial in achieving this objective as they can induce more significant turbulence in the airflow within the heater. Additionally, the literature review indicates that the performance of a double-pass SAH surpasses that of a single-pass SAH. However, it is noted that the utilisation of artificial roughness or baffles in double-pass solar air heaters is notably limited.

Consequently, in the proposed study, a double-pass SAH is employed in conjunction with various artificially created rib arrangements, such as semi-circular and semi-polygonal ribs. The performance of this double-pass SAH is assessed with each rib shape, and comparisons are made with a flat plate to evaluate performance across different configurations. The study comprehensively evaluates and presents the energy, environmental, and economic implications of utilising the double-pass SAH with conventional, semi-circular, and semi-polygonal ribs.

Experimental setup and methodology

Using the design software Solid Works, the DPSAH was modelled. Measurements were taken to be $1000 \times 500 \times 200$ (mm) for the SAH set-up. When modelling, a 2.5-mm-thick plate was used. The length of the duct area was 260 mm, with an angle of 51°. The 40-mm diameter of the blower inlet pipe was intended. The part's flat plate was created and included. Semi-polygon fins are built into the plate. It was modelled at a side of 100 mm and a 45° angle. The polygon's side was estimated to be 100 mm. The plate had semi-circular fins built into it. The half circle's diameter was intended to be 40 mm. Mild steel was used to build the base structure of the SAH system, and aluminium was used to make the collector plate. Aluminium was cost-effective and had a strong thermal conductivity. It is, therefore, regarded as an absorber plate. Over the absorber plate, a single pure glass arrangement was created, serving as a transparent cover. A blower was utilised to supply the SAH system with forced air. Manometer setups were placed at the SAH's inlet and exhaust ports to help measure the pressure drop. K-type thermocouple arrangements were used to measure the various temperatures gleaned from the SAH. Thermocole arrangements are employed at the bottom and sides of SAH systems to stop heat escape from those areas. The schematic diagram of ribs for DPSAH is shown in Fig. 1. The installed SAH system is shown in Fig. 2. The detailed methodology of the proposed study is as follows:

At the Energy Park of the National Engineering College, located in Kovilpatti (latitude: 9.1484° N, longitude: 77.8322° E), a fabricated system was installed to explore solar air heater performance. Extensive analysis of solar radiation patterns in the Kovilpatti area indicated that the proposed location was particularly conducive to solar energy
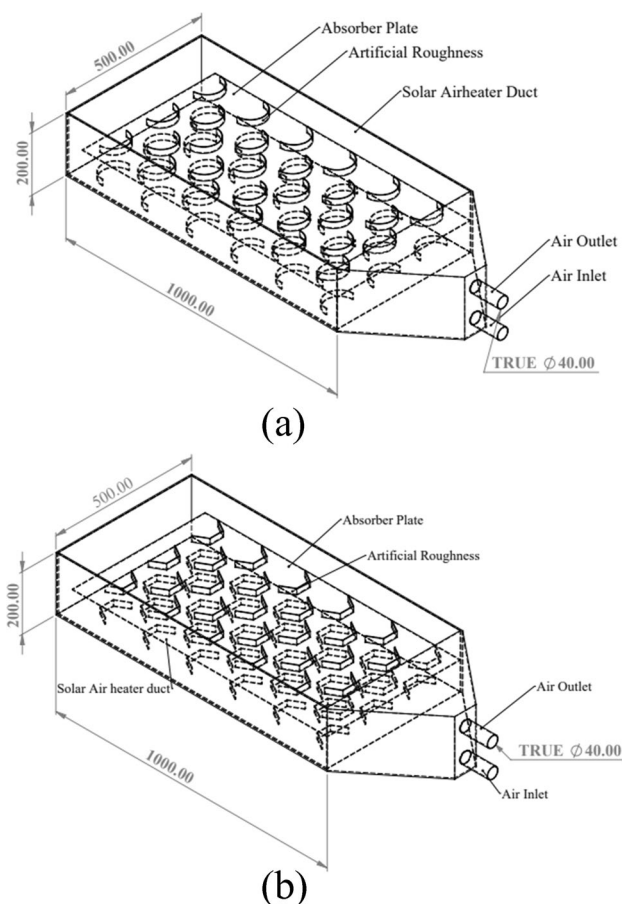

(a)

(b)

Fig. 1 a Schematic diagram of DPSAH with semi-circular fins. **b** Schematic diagram of DPSAH with semi-polygon fins

Fig. 2 DPSAH system installed at the energy park

experimentation. The system was strategically oriented from north to south to optimise solar radiation absorption. Regular measurements of solar radiation levels at the site were conducted every 30 min using a sun meter. Additionally, wind velocity and ambient temperature at the proposed sites were monitored, contributing to system efficiency and top heat loss calculation. Various airflow rates were predetermined based on a comprehensive literature survey. Using a blower, the air was delivered into the DPSAH system at rates of 0.01, 0.02, and 0.03 kg/s. The system's performance metrics, including useful energy output, top heat loss, and overall system efficiency, were evaluated using these three factors: solar radiation, input temperature, and airflow rate. Tests were conducted under similar solar radiation conditions for all three setups: flat plate, semi-circular, and semi-polygon roughness arrangements. Energy output results were meticulously analysed for each set-up, considering the utilisation of black-coated solar absorber plates within the DPSAH. Comparative assessments were made among flat plate, semi-circular, and semi-polygon roughness arrangements, presenting the energy performance of each shape. Furthermore, the system's embodied energy during fabrication was considered to assess the economic and environmental viability of the DPSAH. This holistic approach aimed to provide comprehensive insights into the performance, economic feasibility, and environmental impact of the DPSAH system under study.

Uncertainty analysis

The following equations were employed in error or uncertainty analysis to determine whether errors were made during the experiment and whether the instruments used had errors. Table 1 displays the error value that was obtained.

The equation used to assess mass flow rate uncertainty is

$$\frac{w_{\dot{m}}}{\dot{m}} = \left[\left(\frac{w_{Cd}}{C_d}\right)^2 + \left(\frac{w_A}{A}\right)^2 + \frac{1}{4}\left(\frac{w_{p1}}{P_1}\right)^2 + \left(\frac{w_{\Delta p}}{\Delta P}\right)^2 + \left(\frac{w_{T1}}{T1}\right)^2 \right]^{1/2} \tag{1}$$

The above equation reduces as follows when it is assumed that uncertainty only arises in the measurements of temperature and pressure differential.

Table 1 Uncertainty results

Parameter	Value
Velocity (m/s)	± 0.20
Temperature (°C)	± 2.86
Radiation (W/m²)	± 0.40
Mass flow rate (kg/s)	± 3.8%
Efficiency (%)	± 5.88%

$$\frac{w_{\dot{m}}}{\dot{m}} = \left[\left(\frac{w_{\Delta p}}{\Delta P}\right)^2 + \left(\frac{w_{T1}}{T1}\right)^2 \right]^{4 \, 1/2} \tag{2}$$

When assessing the energy performance, uncertainty arises and is computed using

$$\frac{\omega_\eta}{\eta} = \left[\left(\frac{\omega_m}{m}\right)^2 + \left(\frac{\omega_{\Delta T}}{\Delta T}\right)^2 + \left(\frac{\omega_I}{I}\right)^2 \right]^{1/2} \tag{3}$$

Values obtained using the calculated uncertainty analysis are shown in Table 1.

Energy performance of DPSAH

DPSAH performance was evaluated and compared using the following equations (Rajendran et al. 2021, 2022a, b, 2023).

The density of the solar air heater was found using the following equation:

$$\rho = \frac{P}{RT} \tag{4}$$

where,

P   Ambient pressure in N/m²

R   Gas constant

T   Ambient temperature in K.

The mass flow rate of input air was calculated using

$$\dot{m} = \rho A V \tag{5}$$

where,

ρ Density of air

A   Area of pipe m²

V   Velocity of air m/s.

Solar air heater's heat loss over the top surface was calculated using the equations as follows:

$$U_t = \frac{T_g - T_a}{\frac{1}{A_s(h_r + h_w)}} \tag{6}$$

T_g Average glass cover temperature in K

h_r Radiation heat transfer coefficient on the top surface in W/(m^{2}K).

The radiation heat transfer coefficient can be calculated as follows:

$$h_r = \frac{\sigma(T_{pm}^4 - T_c^4)}{\left(\frac{1}{\epsilon_p} + \frac{1}{\epsilon_c} - 1\right)(T_{pm} - T_c)} \tag{7}$$

$$T_{sky} = T_a - 6 \tag{8}$$

ε_g Glass emissivity

σ Stefan Boltzmann constant value $5.67*10^{-8}$ W/m^2 K^4

T_s Sky temperature

T_a Ambient temperature K.

The empirical relation gives the wind heat transfer coefficient at the top cover (h_w).

$$h_w = 5.67 + 3.86V_w \tag{9}$$

where

V_w Wind velocity m/s.

Useful energy derived from the DPSAH system was evaluated using the following equation:

$$Q = \dot{m}C_p(T_o - T_i) \tag{10}$$

Double-pass solar air heater efficiency was calculated by

$$\eta_{sys} = \frac{Q}{IA} \tag{11}$$

The output performance of the DPSAH system for flat plate, semi-circular, and semi-polygon roughness absorber plates was calculated and compared using the aforementioned equation.

Environmental and economic study

An environmental study is recommended to comprehend the behaviour of DPSAH in producing CO_2, SO_2, and NO emissions to the environment while using the blower and other construction materials. Economic analysis was conducted to determine the DPSAH's payback period and other economic benefits. The system's fabrication cost and the total amount of energy utilised during construction are used to assess the system's economic and environmental performance. It is assumed that the system will last 20 years. The initial fabrication expense is Rs. 20,000.

The economic and environmental behaviour of the system is assessed using the following equations (Singh and Tiwari 2016; Vignesh Kumar et al. 2023):

$$Energy\,Payback\,Time\,(EPT) = \frac{E_{in(KWh)}}{E_{out}\left(\frac{KWh}{Year}\right)} \tag{12}$$

$$Energy\,Production\,Factor\,(EPF) = \frac{E_{out}}{E_{in}} \times T_L \tag{13}$$

$$Life\,Cycle\,Conversion\,Efficiency\,(LCCE) = \frac{\left(E_{out} \times T_L\right) - E_{in}}{\left(E_{sol} \times T_L\right)} \tag{14}$$

$$Annual\ Co_2\ emission = E_{in} * 1.58 \tag{15}$$

$$NO\ emission\ for\ lifetime = E_{in} * 0.005 \tag{16}$$

$$SO_2\ emission\ for\ lifetime = E_{in} * 0.012 \tag{17}$$

$$\text{The } CO_2 \text{ mitigation (kg of } CO_2) \text{ per year} = E_{out} \times 1.58. \tag{18}$$

$$CO_2\ \text{mitigation kg of } CO_2\ \text{over lifetime} = E_{out} \times n_{sys} \times 1.58. \tag{19}$$

$$Net\ CO_2\ \text{mitigation of } CO_2\ \text{over lifetime} = \left(E_{out} \times n_{sys} - E_{in}\right) \times 1.58 \times 10^{-3} \tag{20}$$

$$\text{Carbon credit earned by SAH} = \text{Net CM for lifetime} * 9.99 \tag{21}$$

Environmental expenses are another name for earned carbon credits. Based on the worldwide carbon price per tonne of CO_2 of 11.09 EUR or 9.99 USD, the net CO_2 mitigation total can be traded on the global market.

$$Cost\,of\,yield, C = \frac{TAC}{TAY} \tag{22}$$

TAC   Total annual cost

TAY   Total accumulated yield over time

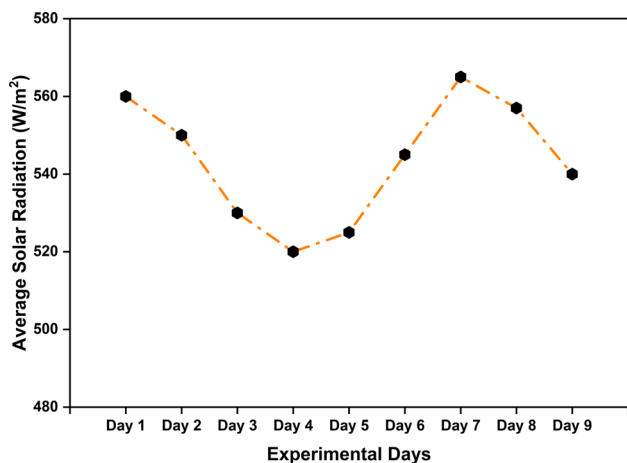$$TAC = FAC + AMC - ASC \tag{23}$$

FAC   Fixed annual cost

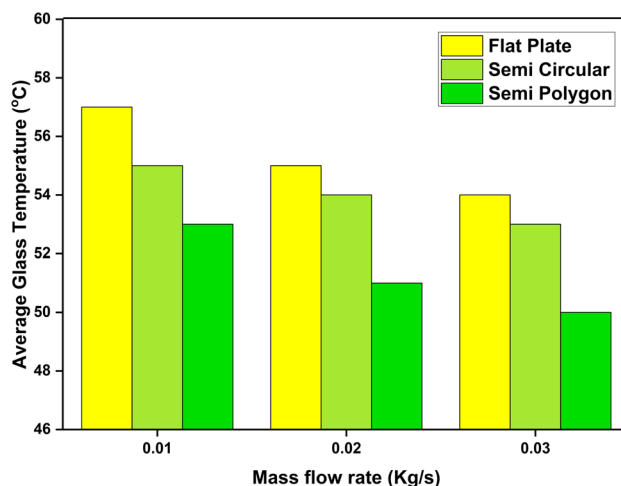Fig. 3 Average solar radiation during trails

AMC   Annual maintenance cost

ASC   Annual salvage cost.

Where, $FAC = PCC * CRF$

$$CRF = \frac{i(1+i)^n}{(1+i)^n - 1'} \qquad (24)$$

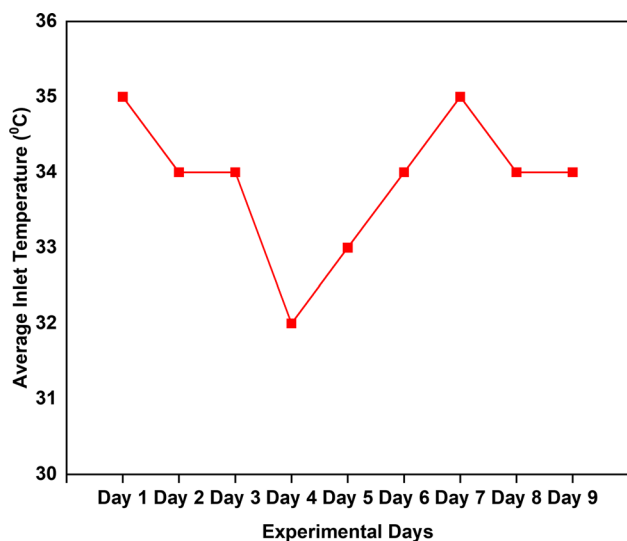$$AMC = 0.05 * FAC \qquad (25)$$

$$ASC = S * SFF \qquad (26)$$

Fig. 4 Average inlet temperature during experimental days

Fig. 5 Average glass temperature for different mass flow rates

$S \quad 0.2 * PCC$

$$SFF = \frac{i}{(1+i)^n - 1'} \qquad (27)$$

$$P_{mr} = R * \frac{(i+1)^n - 1}{i(i+1)^n} \qquad (28)$$

$$P_r = R_{10} * \left[\frac{1}{(i+1)^{10}}\right] + R_{15}\left[\frac{1}{(i+1)^{15}}\right] + R_{20}\left[\frac{1}{(i+1)^{20}}\right] \qquad (29)$$

P_{mr} Maintenance and repair costs

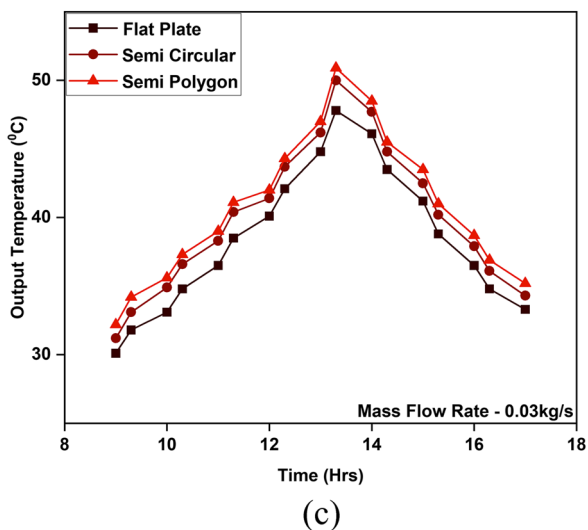P_r Replacement costs
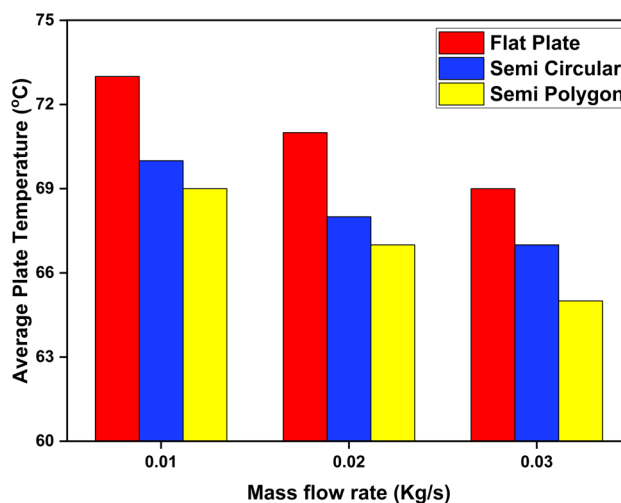
Fig. 6 Average plate temperature for air flow rates

Fig. 7 **a** Output temperature of air vs. time for 0.01 kg/s. **b** Output temperature of air vs. time for 0.02 kg/s. **c** Output temperature of air vs. time for 0.03 kg/s
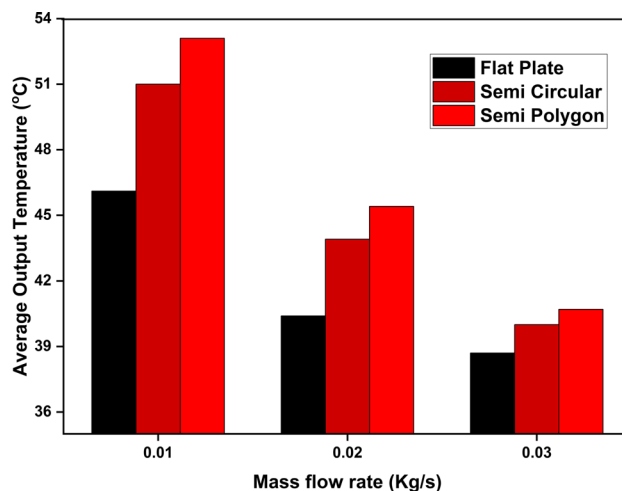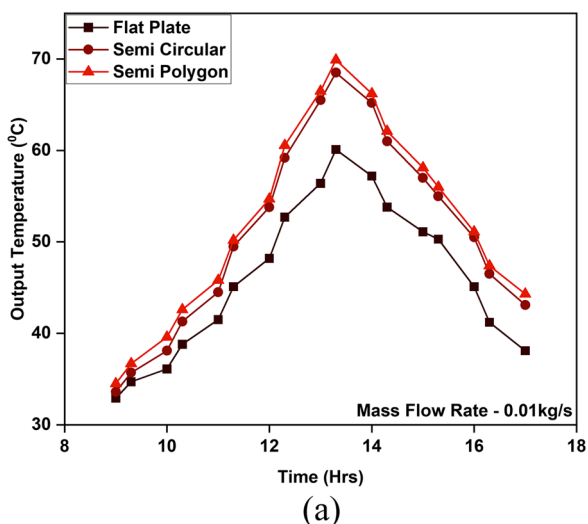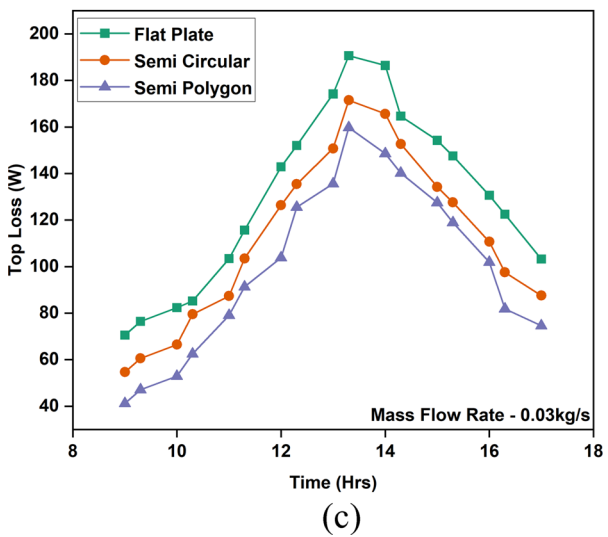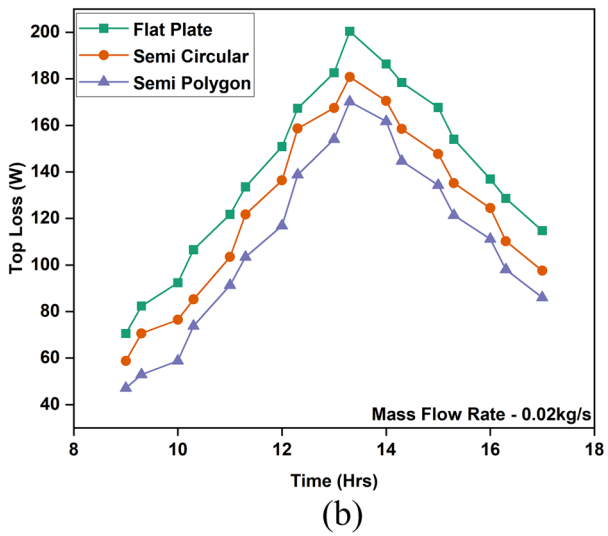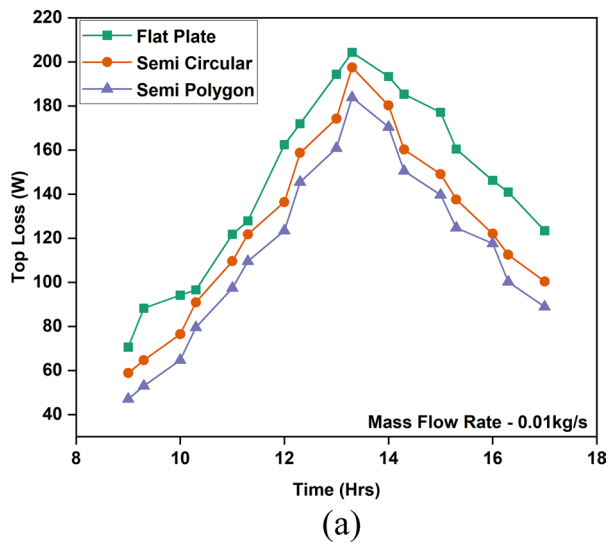
Fig. 8 Average output temperature for mass flow rates
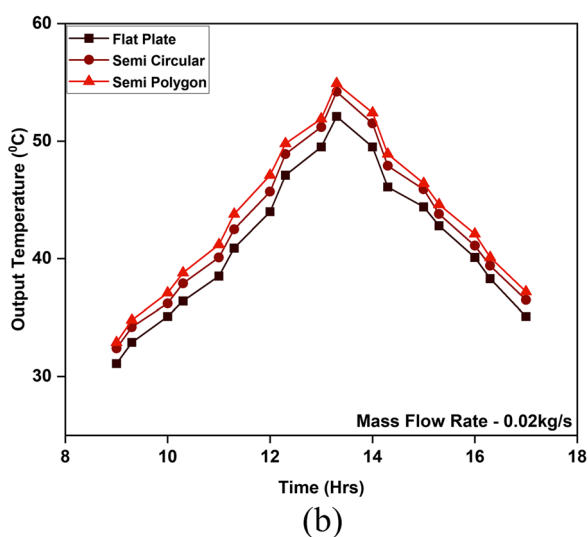
$$P_s = S * \left[\frac{1}{(i + 1)^n} \right] \qquad (30)$$

P_s Salvage value

Net present value $P_{net} = P + P_{mr} + P_r - P_s$ (31)

Results and discussion

The key factor influencing the performance of the SAH is the site at which they are installed. The intended area must receive enough solar radiation for any solar system to function. By absorbing the heat energy from solar radiation, SAH transforms the heat energy into productive work. Experiments with the proposed DPSAH system are conducted in the National Engineering College's energy park in Kovilpatti, South Tamil Nadu. A study of the annual average radiation levels at the suggested site revealed they are suitable for the trials. In April, experiments are conducted, and the device's response to incoming radiation is examined. Experiment trials are run with the required radiation levels from 9.00 AM to 5.00 PM. In the morning, solar radiation is less intense; as the trails continue, it gradually increases. It received far more radiation than normal in the afternoon. Then the radiation started to decrease, as shown in Fig. 3. The experiments got 520 to 558 W/m^2 of solar radiation on average each. The ranges are somewhat comparable and do not deviate much when on the trails. Therefore, the proposed semi-polygonal, semi-circular, and flat plate SAH are tested in these radiation ranges, and their performances are compared.

(a)

(b)

(c)

Fig. 9 **a** Top loss vs. time for 0.01 kg/s. **b** Top loss vs. time for 0.02 kg/s. **c** Top loss vs. time for 0.03 kg/s
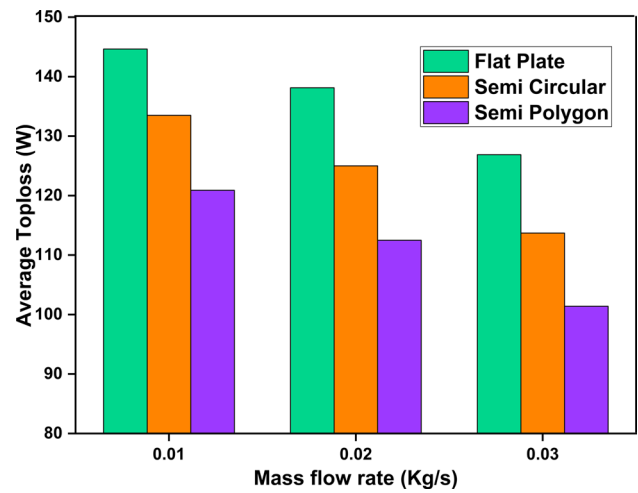

Fig. 10 Average top loss for different air flow rates

During the experiment, different temperatures, including those of the absorber plate, the glass, and the output, are measured to assess the system's heat transfer and thermal performance. The ambient temperature and wind speed are employed as input parameters to determine temperature differences. Figure 4 displays the input air temperature that was sent to the SAH system. The graph demonstrates how the input temperature ranges rise during the course of the experiment, reaching a high value in the late afternoon in relation to solar radiation. During the trials, the average input temperature ranged from 32 to 35 °C.

Since glass temperatures are mainly required to determine a system's top heat loss, this glass ensures long-term sustainability for pure glass, which is used to lower system losses. The temperature of the glass is measured in two places on the transparent glass. The modified SAH has slightly warmer glass than the regular SAH, as shown in Fig. 5. Due to the fact that modified SAH has a significantly higher temperature for convective heat transfer to the air than standard SAH, it also demonstrates that when airflow improves, glass temperature decreases as a result of minimum heat transfer to the air at a higher mass flow rate. For the flat-plate SAH system, the average glass temperatures received are 57 °C, 55 °C, and 54 °C for flow rates of 0.01, 0.02, and 0.03 kg/s. For the same flow rates that were examined, semi-polygonal systems receive average glass temperatures of 53 °C, 51 °C, and 50 °C, whereas semi-circular baffle systems receive average glass temperatures of 55 °C, 54 °C, and 53 °C.

The performance of the SAH system is greatly influenced by the collector plate's temperature. Because it allows heat to be convectively transferred from the hot collector plate to the air that is flowing, the outlet air temperature is higher than the ambient or inlet air temperature. Additionally, because it is painted black, it absorbs more heat from solar radiation, resulting in an absorber plate temperature that is
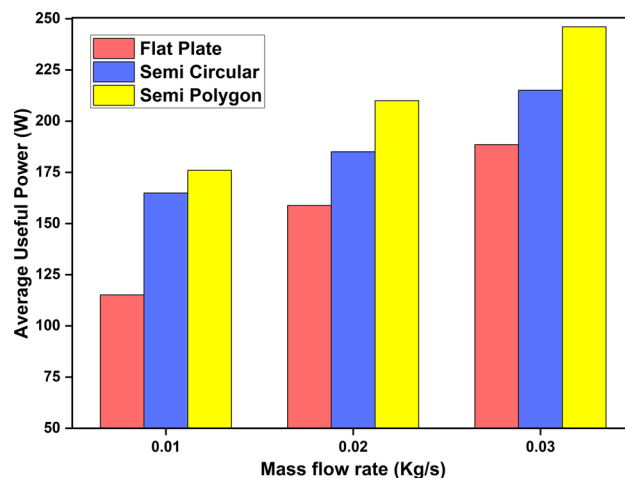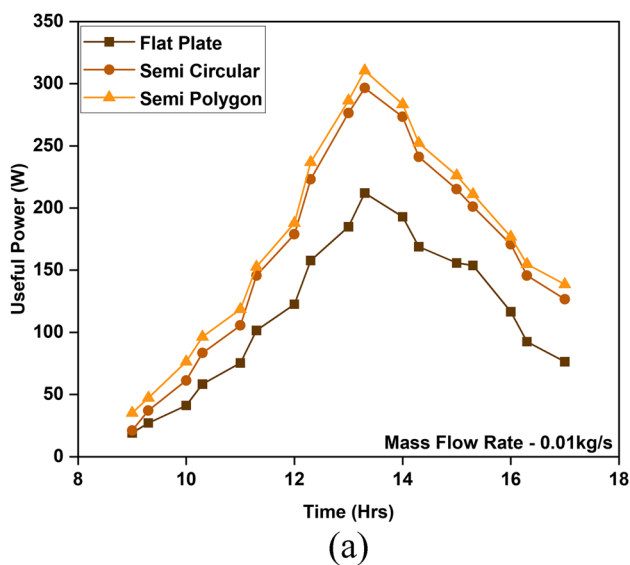
(a)

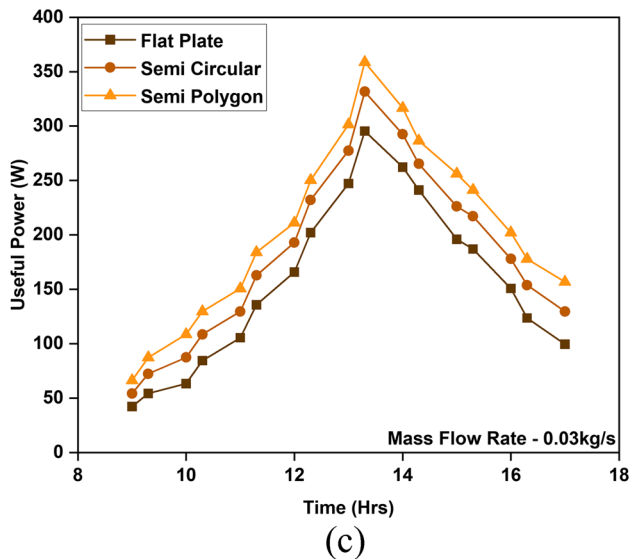**Fig. 12** Average useful power for different mass flow rates
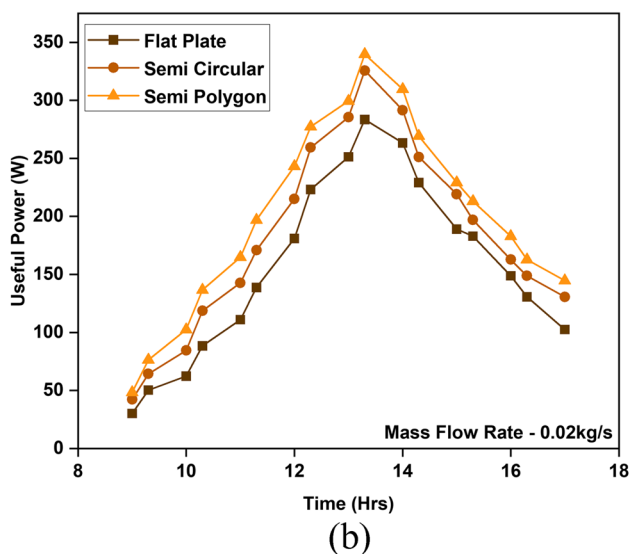

(b)

(c)

Fig. 11 **a** Useful power vs. time for 0.01 kg/s. **b** Useful power vs. time for 0.02 kg/s. **c** Useful power vs. time for 0.03 kg/s

higher than glass temperature. Because there is more excellent heat transfer in the DPSAH with baffles than in the flat-plate DPSAH, the temperature of the absorber plate is higher in the flat-plate DPSAH. Figure 6 displays the absorber plate temperature recorded throughout the experiment periods. For flat-plate DPSAH during the studies, the average absorber plate temperatures recorded were 73 °C, 71 °C, and 69 °C for the flow rates of 0.01, 0.02, and 0.03 kg/s. The DPSAH systems provided 70 °C, 68 °C, and 66 °C for semi-circular baffle arrangements and 69 °C, 67 °C, and 64 °C for semi-polygon form roughness for the same examined flow rates. It is evident that the roughness arrangement provided improved convective heat transfer compared to a flat plate.

An improved performance of SAH is influenced by the DPSAH's output temperature. For the baffled air heater compared to the conventional one, the surface contact area between the air and the absorber plate is significantly higher. Also, the airflow inside the SAH system is controlled by baffles being placed over the absorber plate in the DPSAH. As a result, the system's air flow becomes much more turbulent, which increases the air flow's retention duration inside the SAH and enhances convective heat transfer. The experiment's output temperature is depicted in Fig. 7. For the air flow rates of 0.01, 0.02, and 0.03 kg/s, the average output temperatures of flat-plate DPSAH are 46.1, 40.4, and 38.7 °C. Semi-circular DPSAH yields 51, 43.9, and 40 °C while semi-polygon baffles DPSAH offers 53.1, 45.4, and 40.8 °C for the same examined flow rates shown in Fig. 8. The graph clearly shows that air flow rates directly affect output temperatures, with higher flow rates resulting in lower output temperatures. Additionally, it demonstrates that during the trial, the semi-polygon DPSAH system gives a higher output temperature. It produces output temperatures that are 15.18, 12.37, and 5.4% higher than flat plate DPSAH and 4.11, 3.41, and 2% higher than semi-circular DPSAH.
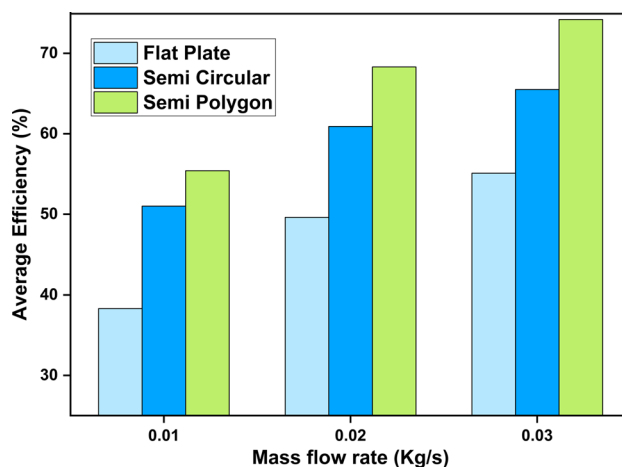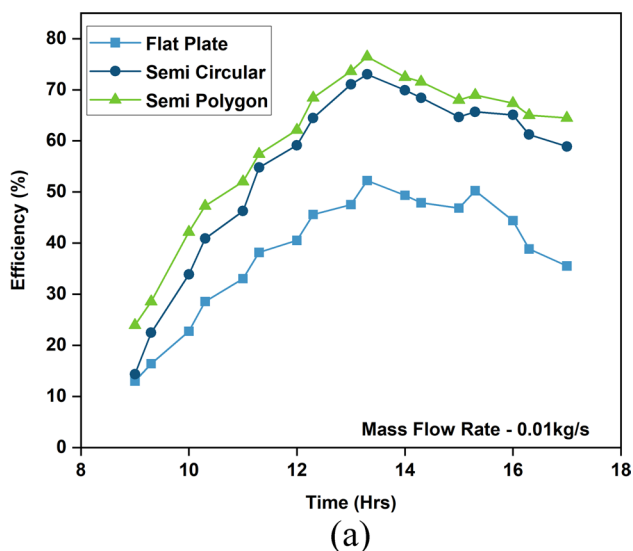
(a)

(b)

(c)

Fig. 13 **a** Efficiency vs time for 0.01 kg/s. **b** Efficiency vs time for 0.02 kg/s. **c** Efficiency vs time for 0.03 kg/s
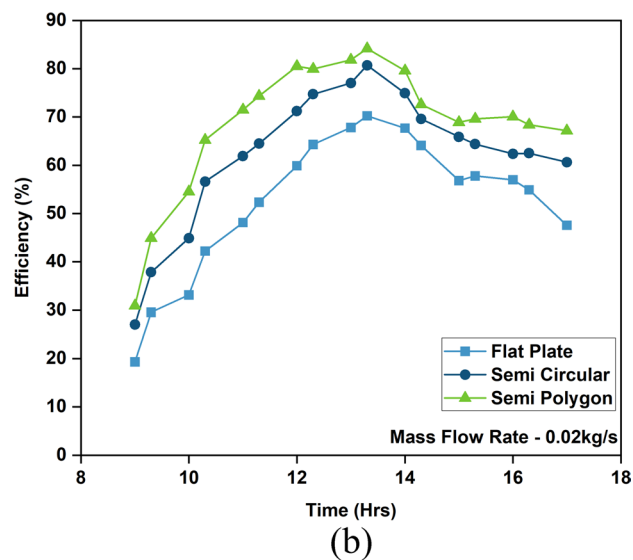
Fig. 14 Average efficiency for different mass flow rates

The SAH system input is calculated using the total energy received from the solar across the entire collector area. A portion of the total solar input is turned into useful energy, which is used to assess system efficiency. A portion of the remaining energy is lost as a top loss from the system, leaving the remainder as an unaccounted loss. A solar air heater's efficiency is significantly impacted by its top loss since insulation lowers side and bottom loss. The distribution of incident solar radiation's energy between top loss and energy gain is controlled by the heat balance of the air heater. According to graph 9, a conventional air heater has a more enormous top heat loss than an SAH with a baffle (Fig. 9).

Additionally, when glass temperature rises, more heat is lost to the environment via convection and radiation. Due to the higher glass temperatures of conventional air heaters compared to baffled air heaters, traditional air heaters waste more heat from the system. Additionally, because of internal diffraction between the collector surface and glass, the enhanced SAH reduces the amount of solar radiation that is reflected back to the outside. For air flow rates of 0.1, 0.02, and 0.03 kg/s, the average top losses of a conventional DPSAH system are 144.64, 135.14, and 124.89 W, which are 8.34, 9.86, and 11.8% higher than the average heat loss from the top of a semi-circular DPSAH system and 19.63, 22.29, and 25.64% higher than that of a semi-polygonal DPSAH system as shown in graph 10 (Fig. 10). Due to the fact that for the tested flow rates, semi-circular DPSAH only delivers 133.5, 123, and 111.7 W, while semi-polygon DPSAH only offers 120.9, 110.5, and 99.4 W of average top loss.

The differential in air temperature between the input and output, as well as the airflow rate, determines DPSAH's useful power. The air circulating duration inside the SAH absorber increases as the mass flow rate is kept to a minimum. By raising the temperature of the output air, this helps

Table 2 Results of comparative study

| Authors	Modifications	Flow rates	Outcome
(Fudholi et al. 2013)	DPSAH with fin arrangements	0.01–0.1 kg/s	Maximum thermal efficiency, 77%
(Dhiman and Singh 2015)	DPSAH with recycled air and wire mesh	0.01–0.025 kg/s	Maximum thermal efficiency, 80.8%
(Abdullah et al. 2018)	DPSAH with turbulator	0.02 to 0.05 kg/s	Average efficiency, 68%
(Baig and Ali 2019)	DPSAH with four copper conduits and paraffin wax	0.05 kg/s	Maximum efficiency, 97%
(Abo-Elfadl et al. 2020)	DPSAH with aluminium tubes	0.025, 0.05, and 0.075 kg/s	Efficiency 40.3% higher than flat-plate DPSAH
(Abo-Elfadl et al. 2021)	DPSAH with tubular absorber	0.025, 0.05, and 0.075 kg/s	Maximum efficiency, 86%
(Hassan et al. 2022)	DPSAH with V groove	0.021–0.061 kg/s	Maximum thermal efficiency, 88.8%
(Raturi et al. 2022)	DPSAH with V-shaped baffles	0.02 kg/s	Efficiency 33.7% higher than flat-plate DPSAH
Proposed work	DPSAH with semi-polygonal ribs	0.01, 0.02, and 0.03 kg/s	Maximum average efficiency, 74.2%
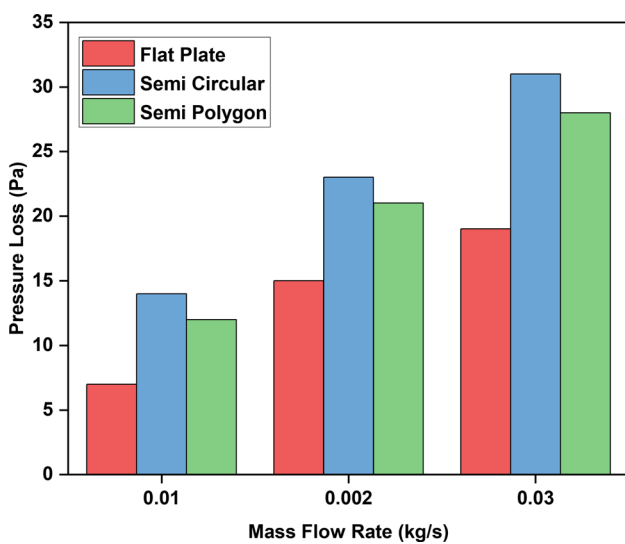
Fig. 15 Pressure drop for different mass flow rates

Table 3 Results of the environmental study

Parameter	Semi-circular	Semi-polygon
Energy output (E_{out})	784.85	898.19
Embodied energy (kWh) (E_{in})	1512.07	1527.21
Energy payback time (EPF)	1.926571956	1.700319532
Energy production factor (EPF)	0.519056657	0.58812475
Life cycle conversion efficiency (LCCE)	27.81	39.05
CO_2 emission (kg)	2389.0706	2412.9918
SO_2 emission for lifetime (kg)	18.14484	18.32652
NO emission for lifetime (kg)	7.56035	7.63605
CO_2 mitigation	22,412.1894	25,969.8122
CO_2 mitigation (tons)	99.59	125.17
Carbon credit earned (INR)	99,490.41	125,044.83
Carbon credit earned ($)	895.65	1125.70

to boost the rate of convective heat transfer. A maximum output temperature and optimum mass flow rate will enhance the useful energy gain. DPSAH's useful power rises as time duration rises and reaches its peak in the late afternoon, much like solar radiation levels. The useful power provided by the DPSAH with a flat plate and suggested roughness arrangements is shown in Fig. 11. For air flow rates of 0.01, 0.02, and 0.03 kg/s, flat-plate DPSAH produces average useful powers of 115.1, 148.8, and 188.5 W, semi-circular DPSAH produced 144.87, 180.05, and 215.03 W, and semi-polygon DPSAH produced 175.96, 209.94, and 246.08 W as shown in graph 12 (Fig. 12). Semi-polygon arrangements provide 21.4, 16.60, and 14.43% more average useful power than semi-circular DPSAH, while for the same flow rate, they supply 52.87, 41.04, and 30.54% more useful power than flat-plate DPSAH. It is evident that semi-polygonal configurations, which offer more outstanding convective heat transfer than semi-circular and flat-plate DPSAH, boost the useful power ranges above those of the former due to the improved turbulent flow inside the SAH system.

The DPSAH efficiency is used to express the percentage of incident energy that is converted into useful energy gain at an outlet. An efficiency assessment takes into account the air flow rate, solar radiation, temperature differences between the input and output, and collector area. The air going through SAH with a baffle retains air for a significantly longer period of time than SAH with a flat surface. By doing this, the air and absorber plate can transfer heat more effectively. Owing to the turbulentof air activity in the SAH and the presence of baffles, the creation of the laminar flow in the absorber plate is limited. This method effectively increases efficiency and convective heat transfer. Figure 13 illustrates the effectiveness of flat and suggested roughness layouts for various flow rates. It is evident that increasing airflow rates results in increased efficiency, with a higher flow rate system achieving the maximum efficiency. The

Table 4 Results of the economic study

Various Costs	Semi-circular			Semi-polygon		
	$n = 10$ yrs	$n = 15$ yrs	$n = 20$ yrs	$n = 10$ yrs	$n = 15$ yrs	$n = 20$yrs
Capital recovery factor	0.162	0.13	0.11	0.162	0.131	0.117
Sinking factor fund	0.062	0.031	0.017	0.062	0.031	0.017
Annual fixed cost ($)	54.63	44.13	39.43	54.63	44.13	39.43
Annual maintenance cost ($)	5.46	4.41	3.94	5.46	4.41	3.94
Salvage value ($)	67.14	67.14	67.14	67.14	67.14	67.14
Annual salvage value ($)	4.21	2.11	1.17	4.21	2.11	1.17
Annualised cost ($)	55.8	46.4	42.2	55.8	46.4	42.2
Annual cost (kWh, $)	5.18	4.31	3.91	5.93	4.93	4.48
Net present value ($)	**421.42**			**466.13**		

average system efficiency is shown in Fig. 14. For air flow rates of 0.01, 0.02, and 0.03 kg/s, the average efficiencies of flat-plate DPSAH are 38.3, 49.6, and 55.1%. For the same flow rates, semi-circular DPSAH produced 51, 60.9, and 65.5%, and semi-polygon arrangements produced 55.4, 68.3, and 74.2% average system efficiency. Semi-polygon roughness performs better than semi-circular DPSAH and flat-plate DPSAH in every way, with 17.1, 18.7, and 19.1% greater average efficiency than the flat plate and 4.4, 7.4, and 8.7% higher average efficiency than semi-circular DPSAH.

To prove the suitability of the proposed work, a comparison with previously published works has been done. The findings demonstrate that the suggested DPSAH configurations with semi-polygonal ribs have equivalent performance to the earlier research. Table 2 displays the findings obtained from the comparative investigation.

Finding the pressure loss ranges is vital since system pressure loss significantly impacts how well the system performs with SAH. The pressure loss experienced during the SAH experiment for the flat plate, semi-circular, and semipolygon DPSAH is shown in Fig. 15. The pressure loss inside the solar air heater is improved by adding baffles over the absorber plate. The graph makes it abundantly clear that increased air flow rates result in more significant pressure loss for flat- and baffled-air heaters. However, compared to DPSAH systems, the useful power obtained from the pressure loss ranges is relatively low, which has no impact on the system for the suggested shape.

Table 3 displays the results of environmental research that was carried out utilising DPSAH and a semi-circular and semi-polygonal rib configuration. The findings indicate that semi-polygonal ribs have a shorter payback period, a higher energy production factor, and a more efficient life cycle compared to semi-circular ribs.

Table 4 lists the financial gains made possible by the system analysis. The suggested DPSAH with semi-circular and semi-polygonal ribs clearly has economic advantages based on the findings of the economic study. However, semi-polygonal ribs also perform better economically than

semi-circular ribs. It has a significant net present value over the course of its lifetime compared to semi-circular ribs and an annual cost related to energy output.

Conclusions

According to the DPSAH trials, semi-polygonal rib arrangements exceed other shapes for the same location in terms of energy performance. It also demonstrates how much more energy was gained, efficiency increased, and output temperature decreased due to the increased air flow rates.

- In contrast to the conventional DPSAH, the SAH's inclusion of semi-circular ribs and semi-polygonal ribs improved turbulence within the SAH, which improved convective heat transfer between the absorber plate and air.
- An average output temperatures of the DPSAH with semi-polygonal ribs were 15.18, 12.37, and 5.4% higher than flat plate DPSAH and 4.11, 3.41, and 2% higher than semi-circular DPSAH according to the findings.
- Due to this enhancement in heat transfer, DPSAH with semi-polygonal ribs produced average efficiencies that were 17.1, 18.7, and 19.1% higher than those of flat plates and 4.4, 7.4, and 8.7% higher than those of semi-circular DPSAH.
- Additionally, it offers 52.87, 41.04, and 30.54% more useful power than flat plate DPSAH and 21.4, 16.60, and 14.43% higher average useful power than semi-circular DPSAH.
- DPSAH systems with flat-plate surface have 8.34, 9.86, and 11.8% higher average heat loss from the top surface than the semi-circular DPSAH system and 19.63, 22.29, and 25.64% higher than that of a semi-polygonal DPSAH system.
- These semi-polygonal ribs also have lower top loss values than the semi-circular and flat-plate DPSAH.

Future studies can evaluate these designs for single-pass SAH, with storage and various nanocoatings over the absorber plate.

An experimental investigation integrating energy storage materials and investigating different absorber plate coatings for the double-pass solar air heater (DPSAH) is planned for the future.

Author contribution RVK contributed to evaluating solar air heater performance and writing the manuscript, RV contributed to fabrication of the solar air heater, and PM contributed in validation of the results and discussion.

Data availability The datasets used and analysed during the current study are available from the corresponding author upon reasonable request.

Declarations

Ethical approval Not applicable.

Consent to participate All the individual participants involved in the study have provided informed consent.

Consent to publish The participant has consented to submitting the study to the journal.

Competing Interests The authors declare no competing interests.

References

Abdullah AS, Abou Al-sood MM, Omara ZM et al (2018) Performance evaluation of a new counter flow double pass solar air heater with turbulators. Sol Energy 173:398–406. https://doi.org/10.1016/j.solener.2018.07.073

Abo-Elfadl S, Hassan H, El-Dosoky MF (2020) Study of the performance of double pass solar air heater of a new designed absorber: an experimental work. Sol Energy 198:479–489. https://doi.org/10.1016/j.solener.2020.01.091

Abo-Elfadl S, Yousef MS, Hassan H (2021) Energy, exergy, and enviroeconomic assessment of double and single pass solar air heaters having a new design absorber. Process Saf Environ Prot 149:451–464. https://doi.org/10.1016/j.psep.2020.11.020

Alam T, Kim MH (2017) Performance improvement of double-pass solar air heater – a state of art of review. Renew Sustain Energy Rev 79:779–793

Aldabbagh LBY, Egelioglu F, Ilkan M (2010) Single and double pass solar air heaters with wire mesh as packing bed. Energy 35:3783–3787. https://doi.org/10.1016/j.energy.2010.05.028

Baig W, Ali HM (2019) An experimental investigation of performance of a double pass solar air heater with foam aluminum thermal storage medium. Case Stud Therm Eng 14. https://doi.org/10.1016/j.csite.2019.100440

Chamoli S, Chauhan R, Thakur NS, Saini JS (2012) A review of the performance of double pass solar air heater. Renew Sustain Energy Rev 16:481–492

Dhiman P, Singh S (2015) Recyclic double pass packed bed solar air heaters. Int J Therm Sci 87:215–227. https://doi.org/10.1016/j.ijthermalsci.2014.08.017

Fudholi A, Sopian K, Ruslan MH, Othman MY (2013) Performance and cost benefits analysis of double-pass solar collector with and without fins. Energy Convers Manag 76:8–19. https://doi.org/10.1016/j.enconman.2013.07.015

Gabhane MG, Kanase-Patil AB (2017) Experimental analysis of double flow solar air heater with multiple C shape roughness. Sol Energy 155:1411–1416. https://doi.org/10.1016/j.solener.2017.07.038

Hassan H, S. Yousef M, Abo-Elfadl S (2021) Energy, exergy, economic and environmental assessment of double pass V-corrugated-perforated finned solar air heater at different air mass ratios. Sustain Energy Technol Assess 43. https://doi.org/10.1016/j.seta.2020.100936

Hassan A, Nikbahkt AM, Welsh Z et al (2022) Experimental and thermodynamic analysis of solar air dryer equipped with V-groove double pass collector: techno-economic and exergetic measures. Energy Convers Manag X 16. https://doi.org/10.1016/j.ecmx.2022.100296

Ho CD, Lin CS, Chuang YC, Chao CC (2013) Performance improvement of wire mesh packed double-pass solar air heaters with external recycle. Renew Energy 57:479–489. https://doi.org/10.1016/j.renene.2013.02.005

Khanlari A, Tuncer AD (2023) Analysis of an infrared-assisted triple-flow prototype solar drying system with nano-embedded absorber coating: an experimental and numerical study. Renewable Energy 216:119125. https://doi.org/10.1016/j.renene.2023.119125

Khanlari A, Badali Y, Tuncer AD (2023) Analysis of a spiral-formed solar air heating system with ceria nanoparticles-enhanced absorber coating. J Build Eng 71:106534. https://doi.org/10.1016/j.jobe.2023.106534

Kumar A, Akshayveer SAP, Singh OP (2020) Efficient designs of double-pass curved solar air heaters. Renew Energy 160:1105–1118. https://doi.org/10.1016/j.renene.2020.06.115

Mahmood AJ, Aldabbagh LBY, Egelioglu F (2015) Investigation of single and double pass solar air heater with transverse fins and a package wire mesh layer. Energy Convers Manag 89:599–607. https://doi.org/10.1016/j.enconman.2014.10.028

Murali G, Sai Nandan B, Sampath Kumar Reddy N et al (2020) Experimental study on double pass solar air heater with fins at lower and upper channel. In: Materials Today: Proceedings. Elsevier Ltd, pp 578–583

Prakash O, Kumar A, Samsher et al (2022) Exergy and energy analysis of sensible heat storage based double pass hybrid solar air heater. Sustain Energy Technol Assessments 49. https://doi.org/10.1016/j.seta.2021.101714

Rajendran V, Ramasubbu H, Alagar K, Ramalingam VK (2021) Performance analysis of domestic solar air heating system using V-shaped baffles – an experimental study. Proc Inst Mech Eng Part E J Process Mech Eng 235:1705–1717. https://doi.org/10.1177/09544089211016256

Rajendran V, Ramasubbu H, Rajarathinam JV, Pichandi R (2022a) Experimental study on the thermal performance of a solar air heater integrated with multi-geometry arrangements over the absorber plate. Environ Sci Pollut Res 29:38331–38345. https://doi.org/10.1007/s11356-022-18830-x

Rajendran V, Singaraj K, Rajarathinam J (2022b) Environmental, economic, and performance assessment of solar air heater with inclined and winglet baffle. Environ Sci Pollut Res. https://doi.org/10.1007/s11356-022-23213-3

Rajendran V, Vikram MP, Kim SC et al (2023) Enhancing the performance of a solar air heater by employing the broken V-shaped ribs. Environ Sci Pollut Res. https://doi.org/10.1007/s11356-023-27814-4

Ramalingam Vignesh Kumar, Rajendran Vijayakumar, Rajarathinam Jaya Venkatesh (2023) An efective solar assisted semi-cylindrical

saline water desalination system with direct atomiser and energy storage materials for domestic use: an experimental investigation. Environ Sci Pollut Res. https://doi.org/10.1007/s11356-023-30896-9

Raturi P, Deolal H, Kimothi S (2022) Numerical analysis of the return flow solar air heater (RF-SAH) with assimilation of V-type artificial roughness. Energy Built Environ. https://doi.org/10.1016/j.enbenv.2022.09.002

Ravi RK, Saini RP (2016a) Experimental investigation on performance of a double pass artificial roughened solar air heater duct having roughness elements of the combination of discrete multi V shaped and staggered ribs. Energy 116:507–516. https://doi.org/10.1016/j.energy.2016.09.138

Ravi RK, Saini RP (2016b) A review on different techniques used for performance enhancement of double pass solar air heaters. Renew Sustain Energy Rev 56:941–952

Sajawal M, Rehman TU, Ali HM et al (2019) Experimental thermal performance analysis of finned tube-phase change material based double pass solar air heater. Case Stud Therm Eng 15. https://doi.org/10.1016/j.csite.2019.100543

Salih SM, Jalil JM, Najim SE (2019) Experimental and numerical analysis of double-pass solar air heater utilising multiple capsules PCM. Renew Energy 143:1053–1066. https://doi.org/10.1016/j.renene.2019.05.050

Singh S, Dhiman P (2016) Thermal performance of double pass packed bed solar air heaters - a comprehensive review. Renew Sustain Energy Rev 53:1010–1031

Singh DB, Tiwari GN (2016) Effect of energy matrices on life cycle cost analysis of partially covered photovoltaic compound parabolic concentrator collector active solar distillation system. Desalination 397:75–91. https://doi.org/10.1016/j.desal.2016.06.021

Sirin C, Tuncer AD, Khanlari A (2023) Improving the performance of unglazed solar air heating walls using mesh packing and nano-enhanced absorber coating: an energy–exergy and enviro-economic assessment. Sustainability 15(21):15192. https://doi.org/10.3390/su152115192

Tandel HU, Modi KV (2022) Experimental assessment of double-pass solar air heater by incorporating perforated baffles and solar water heating system. Renew Energy 183:385–405. https://doi.org/10.1016/j.renene.2021.10.087

Tuncer AD, Khanlari A (2023) Improving the performance of a triple-flow solar air collector using recyclable aluminum cans as extended heat transfer surfaces: an energetic, exergetic, economic and environmental survey. Energy 282:128883. https://doi.org/10.1016/j.energy.2023.128883

Tuncer AD, Amini A, Khanlari A (2023a) Experimental and transient CFD analysis of parallel-flow solar air collectors with paraffin-filled recyclable aluminum cans as latent heat energy storage unit. J Energy Storage 70:108009. https://doi.org/10.1016/j.est.2023.108009

Tuncer AD, Amini A, Khanlari A (2023b) Developing an infrared-assisted solar drying system using a vertical solar air heater with perforated baffles and nano-enhanced black paint. Solar Energy 263:111958. https://doi.org/10.1016/j.solener.2023.111958

Wijeysundera NE, Ah LL, Tjioe LE (1982) Thermal performance study of two-pass solar air heaters. Solar Energy 28(5):363–370. https://doi.org/10.1016/0038-092X(82)90253-5